

Fabrication of Magnetically Separable Mesostructured Silica with an Open Pore System

An-Hui Lu,[†] Wen-Cui Li,[†] Andreas Kiefer,[†] Wolfgang Schmidt,[†] Eckhard Bill,[‡] Gerhard Fink,[†] and Ferdi Schüth^{*,†}

*Max-Planck-Institut für Kohlenforschung, Kaiser-Wilhelm-Platz 1, 45470 Mülheim, Germany, and
Max-Planck-Institut für Bioanorganische Chemie, Stiftstrasse 34-36, 45470 Mülheim, Germany*

Received March 9, 2004; E-mail: schueth@mpi-muelheim.mpg.de

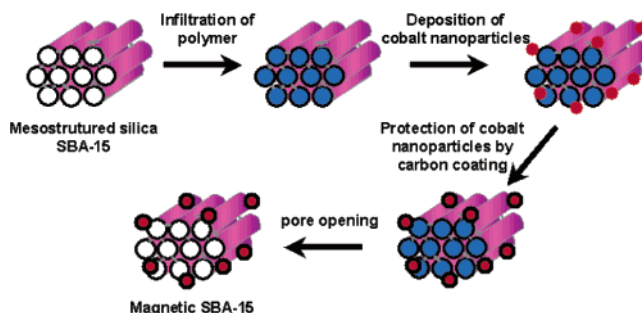
Ordered mesoporous silicas like M41S and the SBA-n series can be synthesized with large surface area, tunable porosity, uniform pore size distribution, and high thermal stability.¹ These materials have application perspectives in heterogeneous catalysis, host–guest chemistry, environmental technology, adsorption, and many other fields.² For many of the envisaged applications, small particle sizes are advantageous, which, however, cause a separability problem in liquid-phase processes.

Magnetic separation provides a convenient method for removal of magnetizable particles by applying an appropriate magnetic field. If one could combine the advantages of mesoporous silica and magnetic particles to fabricate a nanocomposite with high surface area, well-defined pore size, and magnetic separability, a promising novel adsorbent or catalyst support material may be accessible. Attempts to use this strategy have been published before: magnetic nanoparticles of iron oxide or cobalt have been incorporated in the pore system of porous silicas such as MCM-41, MCM-48, and SBA-15.³ However, this often causes clogging of the pore system, which in turn can lead to mass transfer problems. In addition, the occupied pore space restricts further functionalization of the silica inner surface. Moreover, these types of magnetized silicas cannot be used under acidic conditions or at high temperature, since the magnetic particles are not protected against acid erosion or sintering.

We here report a method for fabricating magnetic mesoporous silica with an unobstructed pore system in which the magnetic particles are protected by a nanometer-thick carbon shell against acid erosion. As a model system, SBA-15 was selected as a parent material due to its large pore size and thick pore wall. Cobalt nanoparticles⁴ ca. 10 nm in size were used to impart the magnetic properties to the SBA-15. Syntheses both of SBA-15 and of the cobalt nanoparticles are described in refs 1b and ref 4, respectively.

For the synthesis of the magnetic composite, a strategy was devised as presented in Scheme 1. To exclusively deposit the cobalt nanoparticles on the outer surface of the SBA-15 particles, the pores of SBA-15 should first be blocked with a blocking agent in order to prevent incorporation of the cobalt nanoparticles in the pore system. Subsequently, the cobalt nanoparticles could be grafted on the outer surface of SBA-15. Afterward, the blocking agent needs to be decomposed to recover the pore system. This approach is to some extent related to protection group strategies in organic synthesis, with the difference that not parts of a molecule but rather certain regions in a solid material are temporarily passivated. For the realization of this synthetic scheme, the selected blocking agent needs to be removed completely and easily. On the basis of these considerations, we selected methyl methacrylate (MMA) as the monomer for the blocking agent since poly(methyl methacrylate) (PMMA) is easily decomposed completely below 500 °C.⁵ Thus, after infiltrating SBA-15 with methyl methacrylate monomer and

Scheme 1. Illustration of the Synthesis Pathway for Magnetic Mesostructured Silica



2,2'-azobisisobutyronitrile (AIBN) as an initiator, a PMMA/SBA-15 composite was obtained through polymerization. The composite was impregnated with cobalt nanoparticles suspended in toluene. After drying at 50 °C to remove toluene, the composite was wetted with furfuryl alcohol (FA) solution containing also oxalic acid to initiate polymerization of the FA. Afterward, the composite was treated at 80 °C and then at 850 °C under argon in order to convert the FA into a thin carbon coating on the surface of the cobalt nanoparticles. Simultaneously with the heat treatment to carbonize the poly-FA, the PMMA in the pores of the SBA-15 was decomposed to restore the accessible pore system. This sequence of steps resulted in the formation of magnetic SBA-15, which was denoted as Co/SBA-15-1. A related approach had been developed to prepare a magnetically separable ordered Pd/carbon hydrogenation catalyst.⁶

Alternatively, it might be possible to use the surfactant present in the as-synthesized SBA-15 as the blocking agent. Thus, instead of using calcined SBA-15 as a precursor, the surfactant-containing SBA-15 (Surf/SBA-15) was used after drying at 60 °C under vacuum. Analogous to the procedure described above, the magnetic SBA-15 obtained from Surf/SBA-15 is referred to as Co/SBA-15-2.

Nitrogen sorption isotherms (Figure 1, left) were recorded to assess the textural properties of the samples. The isotherm of Co/SBA-15-1 is of type IV and almost identical to the one of the parent SBA-15, with the volume adsorbed/g reduced due to the extra weight of the added cobalt nanoparticles. The specific surface area and pore volume of Co/SBA-15-1 are 515 m²/g and 0.75 cm³/g, respectively. As seen in the inset, the BJH (Barrett–Joyner–Halenda) pore size distributions of both the original SBA-15 and the Co/SBA-15-1 show an identical distribution. In contrast to that, sample Co/SBA-15-2 shows an isotherm that is markedly different from the normal SBA-15. A visible delayed hysteresis occurs in the relative pressure range of 0.4–0.6, indicating the presence of network percolation effects. This feature has already been observed before for SBA-15 where the mesopores were partially blocked by particles, leading to constrictions in the pore structure.⁷ To exclude

[†] Max-Planck-Institut für Kohlenforschung.

[‡] Max-Planck-Institut für Bioanorganische Chemie.

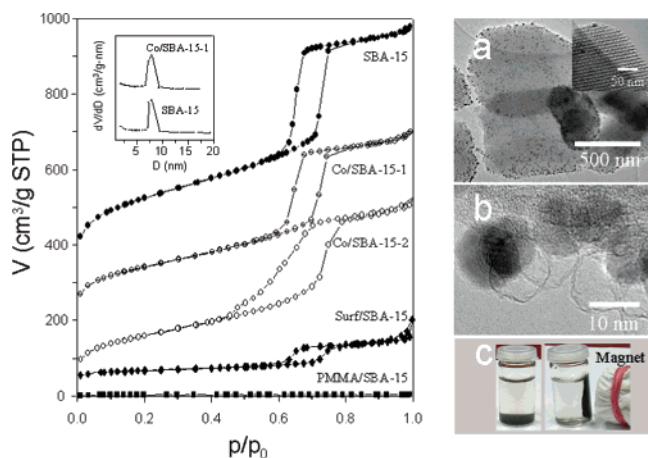


Figure 1. N_2 sorption isotherms and pore size distributions of magnetic silicas and the parent materials (left). The isotherms of Surf/SBA-15, Co/SBA-15-1, and SBA-15 are offset vertically by 50, 200, and 300 $\text{cm}^3 \text{g}^{-1}$ STP, respectively. TEM images (right, a and b) for Co/SBA-15-1 after acid treatment. Magnetically separable Co/SBA-15-1 in water (right, c).

partial pore blocking by carbon residues formed from the surfactant during the thermal treatment as the origin of the delayed condensation, pure Surf/SBA-15 was treated under identical conditions as the Co-containing sample. The dark color of this sample shows that some of the surfactant is converted to carbonaceous material. The nitrogen adsorption isotherm of this sample, however, does not show delayed hysteresis but has a shape identical to that of the calcined SBA-15. This indicates that the small residual amounts of surfactant-derived carbon are present as a thin coating on the pore walls rather than in the form of particles that would block the pore system of SBA-15. Thus, the partial blockage of the pores in Co/SBA-15-2 can be attributed to cobalt particles entering the pores that have a pore size comparable to the diameter of the cobalt particles, despite the presence of surfactant in the pores. As can be seen in Figure 1, a small fraction of the pores of Surf/SBA-15 is not blocked by Pluronic P123, resulting in a small capillary condensation step in the pressure range corresponding to mesopore filling. Therefore, the use of Surf/SBA-15 is disadvantageous if one wants to avoid intrusion of cobalt nanoparticles into the pore system of SBA-15.

In the XRD patterns (Supporting Information), all samples show well-resolved (100), (110), and (200) reflections, indicating that despite the series of treatment steps, all samples still maintain the same structure as the original SBA-15. In the wide-angle range, the reflections characteristic for the fcc cobalt structure are observed; from line-broadening analysis, a size of the cobalt particles of around 10 nm is determined.

To test the acid resistance of the magnetic mesoporous silica, 0.5 g of Co/SBA-15-1 were stored in 500 mL of HCl solution ($\text{pH} = 1$) for 10 days. After filtration, washing with distilled water and ethanol, and drying, the acid-treated sample was characterized using TEM. The TEM image of Co/SBA-15-1 is shown in Figure 1a (right). The morphology of the magnetic mesoporous silica shows the known noodlelike morphology of SBA-15, and the well-dispersed cobalt nanoparticles grafted on the outer surface of the SBA-15 are clearly visible. The size of the cobalt particles is estimated to be ca. 10 nm, which is almost identical to the result based on the XRD measurements. Higher resolution TEM analysis (Figure 1a insert) reveals that the resultant magnetic mesoporous silica exhibits an ordered structure with hexagonal symmetry. A substantial fraction of the cobalt particles survived storage in HCl for more than 10 days, which confirms that these cobalt particles are protected quite well by the carbon shells. In addition, one can

observe the existence of spherulike hollow carbon shells (Figure 1b), which are the result of the dissolution of the cobalt core by HCl solution. This shows that in some cases, the carbon shells do not cover the cobalt particles perfectly to resist acid erosion. Elemental analysis of this sample gives 0.6 wt % carbon and 3.6 wt % cobalt, compared to about 10 wt % cobalt in the parent sample. The residual carbon probably predominantly results from the furfuryl alcohol, which typically gives around 40% carbon yield. It also corresponds roughly to the weight expected for a 0.5–1.0 nm thick carbon coating of the Co particles. The analytical result also demonstrates that PMMA is almost completely decomposed and renders the pore system unobstructed.

The magnetic separability of such magnetic mesoporous silica was tested in a liquid phase by placing a magnet near the glass bottle. As shown in Figure 1c (right), the gray powder is attracted by the magnet, demonstrating that Co/SBA-15 possesses magnetic properties. This will provide an easy and efficient way to separate and recycle Co/SBA-15 from slurry systems. The cobalt particles are superparamagnetic since no hysteresis was observed at 290 K in the magnetization curve (Supporting Information). The saturation magnetization of the magnetic silica is ca. 15.8 emu/g . Since there is 10% cobalt in the magnetic silica, the saturation magnetization of cobalt nanoparticles is ca. 158 emu/g , which is comparable to the bulk value of 163 emu/g .

In summary, magnetically separable mesostructured silica was designed by using cobalt nanoparticles as magnetic anchors and SBA-15 as a host support. When this strategy was used, the pore system of the obtained magnetic SBA-15 was fully accessible and maintained basically in the same state as that prior to anchoring of the cobalt particles. This opens the pathway for such magnetic material to be functionalized further. For instance, the inner surface of such magnetic material might be modified with desired functional groups for metal ion trapping or catalytic purposes. This technology can also be more generally applied to synthesize other magnetic porous silicas and further inorganic materials with unobstructed pore systems.

Acknowledgment. We are highly grateful to N. Matoussevitch for synthesis of the Co particles and B. Spliethoff for TEM analysis. The authors would like to thank the Leibniz Program and the FCI for support. A.-H. Lu acknowledges the Alexander von Humboldt Foundation for a scholarship.

Supporting Information Available: XRD patterns for magnetic silicas and the parent SBA-15, plot of magnetization vs applied field measured at 290 K, and textural parameters of magnetic silicas and the parent materials (PDF). This material is available free of charge via the Internet at <http://pubs.acs.org>.

References

- (1) (a) Kresge, C. T.; Leonowicz, M. E.; Roth, W. J.; Vartuli, J. C.; Beck, J. S. *Nature* **1992**, *359*, 710. (b) Zhao, D.; Feng, J.; Huo, Q.; Melosh, N.; Fredrickson, G. H.; Chmelka, B. F.; Stucky, G. D. *Science* **1998**, *279*, 548.
- (2) (a) Ciesla, U.; Schüth, F. *Micropor. Mesopor. Mater.* **1999**, *27*, 131. (b) Ying, J. Y.; Mehnert, C. P.; Wong, M. S. *Angew. Chem., Int. Ed.* **1999**, *38*, 56.
- (3) (a) Bourlino, A. B.; Simopoulos, A.; Boukos, N.; Petridis, D. *J. Phys. Chem. B* **2001**, *105*, 7432. (b) Fröba, M.; Köhn, R.; Bouffaud, G.; Richard, O.; Tendeloo, G. *Chem. Mater.* **1999**, *11*, 2858. (c) Gross, A. F.; Diehl, M. R.; Beverly, K. C.; Richman, E. K.; Tolbert, S. H. *J. Phys. Chem. B* **2003**, *107*, 5475.
- (4) Bönemann, H.; Brijoux, W.; Brinkmann, R.; Matoussevitch, N.; Waldöfner, N.; Palina, N.; Modrow, H. *Inorg. Chim. Acta* **2003**, *350*, 617.
- (5) Jang, J.; Lim, B. *Angew. Chem., Int. Ed.* **2003**, *42*, 5600.
- (6) Lu, A.-H.; Schmidt, W.; Matoussevitch, N.; Bönemann, H.; Spliethoff, B.; Tesche, B.; Bill, E.; Kiefer, W.; Schüth, F. *Angew. Chem., Int. Ed.* Accepted for publication.
- (7) Schüth, F.; Wingen, A.; Sauer, V. *Micropor. Mesopor. Mater.* **2001**, *44–45*, 465.

JA0486521